Bulletin de la Société Royale des Sciences de Liège, Vol. 69, 2-3, 2000, pp. 111-135

CHLOROPHYLL *a* FLUORESCENCE AND 800 nm ABSORBANCE CHANGES AS TOOLS FOR PROBING LEAF PHOTOSYNTHESIS

Agu LAISK

About photosynthesis

Several photobiological reactions are known but in most of them light is carrying information. Energetic effect is bearing the major role only in photosynthesis, the well-known general equation of which is the following.

$$CO_2 + H_2O + 8hv \rightarrow CH_2O + O_2 \quad (1)$$

Equation 1 is misleading, because it leaves an impression that O_2 evolves from CO_2. Actually O_2 evolves from water and a less misleading form of the equation would be the following

$$CO_2 + 2H_2O + 8hv \rightarrow CH_2O + H_2O + O_2 , \quad (2)$$

or structurally written as

$$O{=}C{=}O + 2\,[\,H\text{-}O\text{-}H] \rightarrow HO-\underset{\displaystyle OH}{\overset{\displaystyle H}{C}}-H + O{=}O \rightarrow HO-\underset{\displaystyle C}{\overset{\displaystyle C}{C}}-H + H\text{-}O\text{-}H + O{=}O \quad (3)$$

The energetic effect of the process is in breaking the strong O-H and C=O bonds and replacing them by weaker C-C, C-H and C-O bonds. Since the intermediate CO_2H_4 configuration is unstable and cannot be formed, the C-moieties are immediately condensed into bigger molecules in a process evolving H_2O. Thus, from four H involved in the reaction only two will stay in the structure of the formed carbohydrate, while two form water again. Generally speaking, the energetic effect of photosynthesis is hidden in the

Abbreviations: a_{II}, a_I , relative optical cross-sections of PS II and PSI antenna; Cyt b_6f , cytochrome b_6f complex; F, fluorescence yield in the light; F_{md}, pulse-saturated fluorescence yield in the dark; F_m, pulse-saturated fluorescence yield in the light; F_0, (lowest) fluorescence yield in the light-adapted state with open PS II centers; FR, far-red light; J_F, J_O, electron transport rates calculated from fluorescence and O_2 evolution, respectively; OEC, oxygen evolving complex; PAD (Q in equations), absorbed flux density of photosynthetically active photons; PS II and PS I, photosystems II and I; P680, P700, PS II and PSI donor pigments; PQ, plastoquinone; Q_A, Q_B, the primary and secondary quinone acceptors of PS II; q_P, photochemical excitation quenching; q_N, q_E, q_I, nonphotochemical excitation quenching of general, "energy-dependent" and inhibitory type, respectively; r_d, PS II donor side resistance to electron transfer per unit leaf area; Y, maximum (intrinsic) quantum yield of PS II electron transport in relation to total PAD; τ, exponential time constant for electron transfer.

Key words: photosynthesis, chlorophyll fluorescence, absorption at 800 nm

energy level of electron orbitals, which are farer from the nuclei in the configuration of HOCH + O_2 than in the configuration of CO_2 +H_2O, and the difference of the potentials is about 1.2 V.

Reaction 3 can be written more easily than performed in nature. It cannot be carried out by one CO_2, because the compound CO_2H_4 is unstable, but the condensation into 6(CH_2O) or at least 3(CH_2O) must be built into the very mechanism of the CO_2 assimilation reaction. For this reason the biochemical mechanism of CO_2 fixation is based on 3-6C compounds and is rather complicated.

The principle of the Calvin-Benson Cycle of CO_2 fixation and reduction (CRC) is shown in Fig. 1. In this cycle, a double-phosphorylated 5C sugar, ribulose 1,5-bisphosphate (RuBP) serves as CO_2 acceptor. The formed 6C2P intermediate splits immediately into two molecules of a 3C1P compound phosphoglyceric acid (PGA). Both PGA molecules are reduced by addition of 2H to form two glyceraldehyde phosphates (GAP). These are condensed, to form a 6C2P compound fructose 1,6-bisphosphate (FBP) and one H_2O is released. The acceptor RuBP is re-synthesized combining the 3C compounds with 2C moieties split from the 6C sugar with the help of the transketolase enzyme.

The driving force of CRC is double phosphorylation. P_i^{2-} ions placed at opposite ends of a carbon chain repulse, trying to split the chain. This happens when RuBP is carboxylated: the 6C intermediate splits immediately. Something similar is expected to happen when two triosephosphates are condensed to form FBP, however, the latter is rapidly dephosphorylated by fructosebisphosphatase. This makes the process irreversible, driving it in the direction of formation the 6C sugar. Another step where double-phosphorylation is needed is at the reduction of PGA. For going in the direction of reduction, an intermediate double-phosphorylated BPGA is formed with the help of ATP, the BPGA is reduced and simultaneously dephosphorylated. The exergonic effect of dephosphorylation neutralizes the endergonic effect of reduction, allowing the reaction to proceed towards reduction. Two ATP are needed for PGA reduction and 1ATP for double phosphorylation of the 5C1P precursor, to form RuBP. Thus 3ATP are hydrolyzed to fix one CO_2. Reduction of PGA proceeds with the help of NADPH, a carrier of 2e$^-$ as reducing power. Thus, all 4 e$^-$ (or

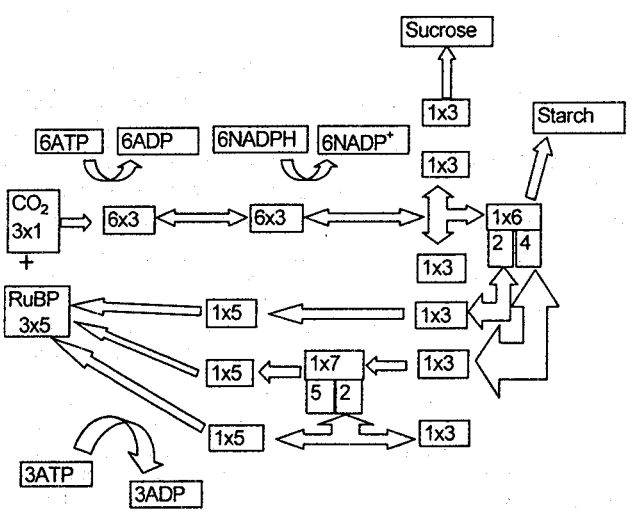

Fig. 1. Principle of conversion of the carbon compounds in the Calvin Benson cycle of carbon reduction (CRC). The number of molecules x the number of C atoms in each molecule are shown per three RuBP carboxylations

equivalent, 4H) detached from 2H_2O are used for 2 PGA reduction.

The above reactions do not need light and for this reason they are called

'dark reactions of photosynthesis'. The energetic cofactors driving the dark reactions, NADPH and ATP are formed in the 'light reactions of photosynthesis', which, as we see, contain only two distinct light steps, the rest of the process going without a need for light energy.

In photosynthesis of plants the reducing power, hydrogen, is generated by splitting water, but it cannot be used in the gaseous form as H_2, but a universal biological carrier of reducing power, NADPH is used for the reduction of PGA in the CRC. To generate NADPH, electrons (e^-) are taken away from water and transported to the oxidized carrier of the reducing power:

$$H_2O + H_2O \rightarrow 4H^+ + 4e^- + O_2 \quad (4)$$

$$2NADP^+ + 4e^- + 4H^+ \rightarrow 2NADPH + 2H^+ \quad (5)$$

Reaction 4 emphasizes that H^+ and e^- stay separated after the splitting of H_2O. Reaction 5 is a summary of e^- transport reactions. It emphasizes that NADPH carries along $2e^-$ but one H^+. Reaction 3 may be rewritten, considering the actual reducing power, as follows

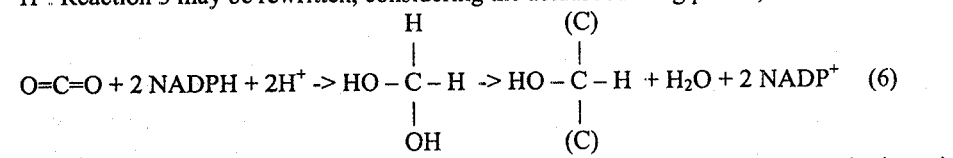

(6)

Reactions 4-6 describe, in a very integrated way, the photosynthetic process beginning with water splitting and ending with the reduction of CO_2 to form a single carbon moiety in a hexose molecule. Optical methods, the topic of our school, can be used to monitor the light reactions that energize reactions 4 and 5.

Light reactions of photosynthesis

Absorbing a photon

Reaction 4, splitting of water, is strongly endergonic and needs input of external energy for going. This energy comes from sunlight.

In order to use a photon for driving photochemical reactions, a molecule must absorb it. In most biochemical compounds where single covalent bonds form the molecules, these bond-forming orbitals are rather close to the nuclei and, correspondingly, the differences between ground and excited energy levels are so high (5-6 V) that most of these compounds absorb ultraviolet light, but not visible light. There is very little UV light in sun radiation, but the spectrum contains much visible light (Fig. 2). Molecules that efficiently absorb visible light, so called pigments, usually contain rather long chains of conjugated bonds. Conjugated chains form like one big orbital farer from the nuclei, which makes the energy difference between the ground and excited states smaller, about 2-3 V, just good for absorption of visible light. The most wide-spread pigment in photosynthesis is chlorophyll, which has a closed circle of conjugated bonds in the pyrrole head. With its first and second excited states Chl absorbs red and blue light, but very little green light (Fig. 3). To fill the gap, Nature has used some accessory pigments, different Chls, like Chl a and Chl b and different Chl-protein interactions, which shift the absorption bands and makes a leaf able to absorb a wider spectrum.

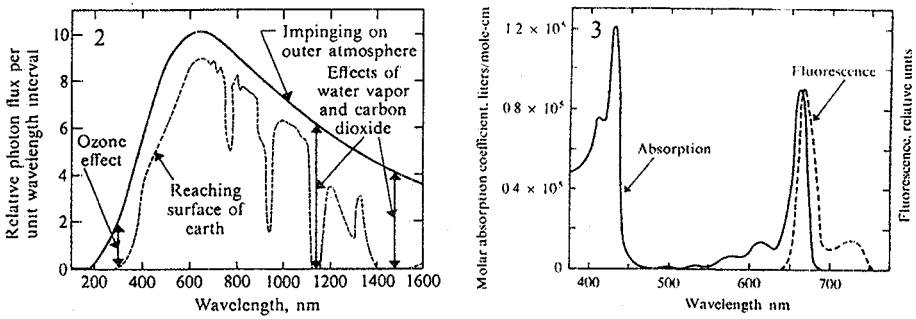

Fig. 2. Wavelength distributions of the sun's photons incident on the earth atmosphere and its surface. From [30]

Fig. 3. Absorption and fluorescence emission spectra of Chl a dissolved in ether. From [30]

Energy storage in photochemical reactions of photosynthesis

When a photon is absorbed by a Chl molecule, one of the π-electrons forming the ring of conjugated bonds jumps to a higher orbital. With this the pigment molecule obtains enormous chemical energy. The excitation potential corresponding to the red absorption band of Chl at 680 nm is 1.8 V. When a mole of Chl becomes excited, their total energy will be 1.8x 96.500 = 173.700 kJ mol^{-1}. Compare this with the average thermal energy of RT=0.008x293 = 2.3 kJ mol^{-1}! Clearly, photochemical energy can reverse the most irreversible reactions, if properly applied.

In solution the excited state of Chl (denoted Chl*) lives about 5 ns and then the excited e^- returns to the ground state. If Chl* meets another compound that has a free ground orbital at a lower energy level than Chl*, e^- may jump over to the neighbor and stay there. If the ground level of the acceptor is still higher than the ground level of the Chl, the difference is saved as chemical energy (Fig. 4).

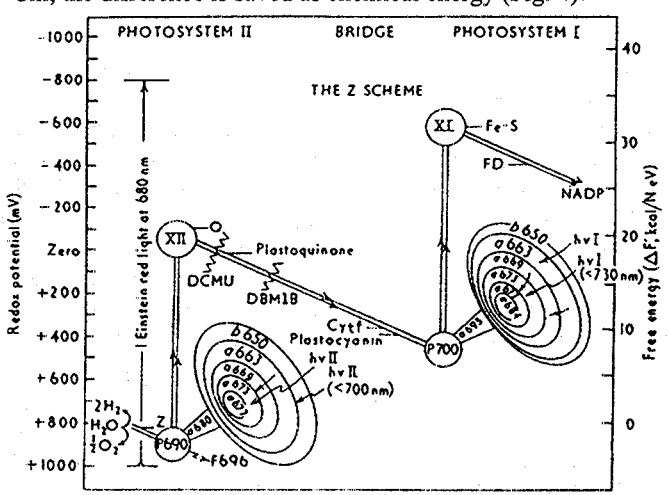

Fig. 4. The Z-scheme, an energy diagram of photosynthesis. From [1]

The probability of the photochemical reaction in Chl solution is a few percent, but it is about 80 % in PSII and 100% in PSI. The reason for such high yield is in biological organization: protein structure holds the donor Chl and acceptor (a quinone denoted Q_A in PSII) close to one another in a right position, to facilitate e^- transfer. As a result of e^- transfer from Chl* to Q_A, the acceptor quinone, Chl^+

cation is formed, which has an exceptionally positive redox potential, being able to oxidize even water. Oxidizing water is energetically very difficult when one or two e^- are taken away from one H_2O. However, when two H_2O are oxidized in concert, so that $4e^-$ are taken away and O_2 is formed at once, the Chl^+ has enough oxidizing power for that. A charge accumulator, accumulating 4 positive charges (missing e^-) is needed to fit the one-e^- transport in photochemistry with the 4-e^- chemistry of oxidizing water. A cluster from 4 Mn atoms can leave 4 e^- in sequence to Chl^+, accumulating 4 positive charges, and the two H_2O react with the Mn^{4+} cluster, liberating O_2. The details of this process are still unknown. Thus, the e^- transport in photosynthesis begins with the excitation and oxidation of Chl, followed by the reduction of the Chl^+ ion from Mn cluster, followed by the reduction of the Mn cluster by water. Beyond PSII, e^- pass through a transport chain consisting of a series of e^- carriers that are able to accept e^- on one hand and to pass it away to the next carrier on the other hand.

There are two light-driven reaction steps in photosynthesis, photosystems II and I (PSII and PSI). The above described water splitting reactions occur on the donor side of PSII. On the acceptor side of PSII, between the two photosystems, e^- are transported by diffusible carriers plastoquinone (PQ) and plastocyanin (PC). Energetically, the interphotosystem e^- transport is going downhill for about 0.4V, but this energy is not totally lost as thermal but is coupled to transport of protons against the electrochemical gradient. The electrochemical H^+ gradient is the driving force for ATP synthesis, which in turn is the driving force for the carbon reduction cycle. Altogether two red photons with the energy of $2x1.8 = 3.6$ V are consumed and, as a result, the e^- is lifted from the ground orbital in H_2O to the ground orbital in NADPH, for about 1.2V. Thus, the theoretically possible maximum energetic efficiency of photosynthesis is $1.2/(2x1.8)=0.33$, when red photons are used. Blue photons, absorbed by the second excitation level of Chl, are rapidly dropped to the first excitation level. Thus, all quanta are truncated to the energy level of red quanta and only the latter is used for photochemistry. For white light the maximum energetic efficiency can be about 0.22.

Harvesting the sun

Though the physical diameter of the Chl head is about 12 Å, its efficient optical diameter is about 1.6 Å (optical cross-section $2.56*10^{-20}$ m^2). For efficient absorption, several hundred layers of Chl have to be placed one behind another in a leaf. For example, in naturally growing birch leaves, Chl concentration is 355 μmol m^{-2}, forming 308 layers of molecules. The protein structure that serves for the light driven e^- transport and H_2O splitting has a molecular weight about 190 kD. It is impossible to build such a structure at every Chl, because the leaf dry mass would be 340 g m^2. First, such a mass of protein would be energetically very expensive to synthesize, second, CO_2 diffusion would be impossible into such thick leaf. Usually leaves have dry mass of 34 g m^{-2}. Such economy has been possible by smartly using physics of excitation transfer between pigment molecules. With the help of light-weight protein structures, about 200 Chl are hold together under certain angles and edge-to-edge distances of a few Å. The collective of Chl is generally called an antenna, but the outer part of it is also called Light Harvesting Complex (LHC). Being so close, excitation can jump from neighbor to neighbor Chl (resonance mechanism), or spread even faster (exciton mechanism). Such a big complex may behave like one big molecule. No matter which molecule absorbs the photon, excitation is shared simultaneously by all Chls. The collective of several tens of Chls behaves like a bell: it can

be excited by hitting any place and the ringing can be quenched by touching any place. There is one (actually a pair) Chl among others that is equipped with the e^- transporting system, named center pigments P680 in PSII and P700 in PSI. When antenna is excited, the excitation is sooner or later (within a picosecond) transferred to the center pigments, where charge separation occurs and excitation is quenched. This way Nature has arranged that several hundred Chls serve one center, P680 in PSII or P700 in PSI (for details see [2-7]).

The above picture is theoretically ideal: one of many Chls around the reaction center absorbs the photon (state Chl*-P680-Q_A-PQ), excitation is rapidly transferred to the center Chl (state Chl-P680*-Q_A-PQ), then oxidized (state Chl-P680$^+$-Q_A^--PQ), the donor side becomes re-reduced from H_2O (state Chl-P680-Q_A^--PQ), e^- is moved away from the acceptor, to the diffusible carrier (state Chl-P680-Q_A-PQ$^-$; when second e^- comes PQ- becomes protonated, diffuses away and is replaced by another, oxidized PQ, state Chl-P680-Q_A-PQH_2 returns to state Chl-P680-Q_A-PQ). In an ideal case such process could be repeated again and again without restrictions, but life is not ideal. Electrons are transported through the e^- transport chain and through PSI to NADP and the formed NADPH is oxidized when CO_2 is reduced. In reality, CO_2 availability depends on stomatal opening, the latter depends on water deficit and other stress factors. Midday sunlight may be too intense for the balanced photosynthetic process. As a result, the next photon may arrive before e^- has left from Q_A^-, because the whole chain until NADPH is reduced, waiting for the next CO_2. What happens when Q_A is still reduced, but excitation is already on Chl*?

Chlorophyll fluorescence

Excitation arrives on P680 as usual, but now a state Chl-P680*-Q_A^--PQH_2 is formed, which does not allow e^- transfer from P680* to Q_A. Excitation returns to the antenna, travels around, revisits P680 several times, but finally becomes quenched other ways than photochemical charge separation. When a Chl is in a solution, excitations may live as long as 5 ns and then, in 70% cases is converted into heat and in 30% cases is emitted as fluorescence. The probability for radiationless conversion of excitation depends on electronic structure of the molecule and on surrounding molecules. Only such pigments can serve for photochemical reactions that have low probability for the thermal conversion of excitation, i.e., where excitation can live long, and Chl is one of these molecules. Usually the probability for thermal conversion increases with the concentration of the pigment, thus the design of the antenna of the photosystems is a problem of optimum: tighter positioning of pigments will increase absorption and fasten excitation transfer between pigments, but the lifetime of excitation will decrease due to increased probability for thermal conversion. This physical phenomenon is efficiently used by plants to control the lifetime of excitation: when photochemistry is unable to use (quench) it, the pigments in the antenna will be moved closer, to facilitate the thermal dissipation of excitation. This way the lifetime of excitation is regulated to about 200-400 ps independent of whether photochemistry can or cannot go fast. In the absence of this nonphotochemical excitation quenching, in the antenna systems of higher plants excitation lifetime is about 2 ns, what is still shorter than in a single Chl in solution. This is the due paid for having the big antenna system, where excitation has to travel [8].

Suppose we have an ideal pigment where thermal dissipation does not occur, will the excitation live forever? No, the excitation is finally emitted as fluorescence, if no other quencher (thermal or photochemistry) was faster to quench it. Fluorescence spectrum is

always shifted to longer wavelengths than the absorption spectrum (Stokes shift), so Chl fluorescence peaks at 680 nm but extends into far-red as far as to 730-760 nm (Fig. 3). Interestingly, at room temperature Chl around PSI (LHCI) emits very little fluorescence, while most of the fluorescence comes from LHCII. At 77K LHCI and LHCII both have high yield of fluorescence. Since photochemistry and fluorescence are competing processes, the quantum yield of fluorescence (ratio of quanta emitted as fluorescence to quanta absorbed) is the higher the lower is the probability for photochemical reaction and thermal conversion. For this reason, probably, PSI fluorescence is very low: evidently in this photosystem charge separation is faster than in PSII. This elementary logic also suggests that Chl fluorescence at PSII can be used to monitor the speed of e^- transport through PSII at room temperatures: when photosynthesis is low, fluorescence is expected to be high and vice versa. This is true and in the following part of this course we look closer, how Chl fluorescence can be used to monitor photosynthetic e^- transport. However, at first we briefly get acquainted with the regulation of the thermal dissipation.

Nonphotochemical quenching of excitation

From the above it is clear that fluorescence yield is expected to be high when light is in excess, i.e., quanta are arriving more frequently than e^- can be accepted by CO_2. From low light about 1-2%, but from high light already 5-10% quanta are re-emitted as fluorescence. This is true, as seen from the recording of fluorescence yield after light was turned high (Fig. 5)

A fluorescence transient contains much information about PSII and such 'fluorescence induction' curves have been thoroughly analyzed. We shall return to the initial, increasing phase of the curve below, but now we notice that fluorescence yield did not remain high under the high light but decreased again, almost to the level as low as in the low light. This complex fluorescence transient was first analyzed by H. Kautsky, and the process is named 'Kautsky effect' [5]. If the light would have been increased to a moderately high level (600-1000 μmol quanta m^{-2} s^{-1}) one could argue that the CO_2 assimilation rate was slowly increasing, due to light-induced enzyme activation. Such light-dependent regulation of CRC enzymes occurs, but in our experiment we applied a

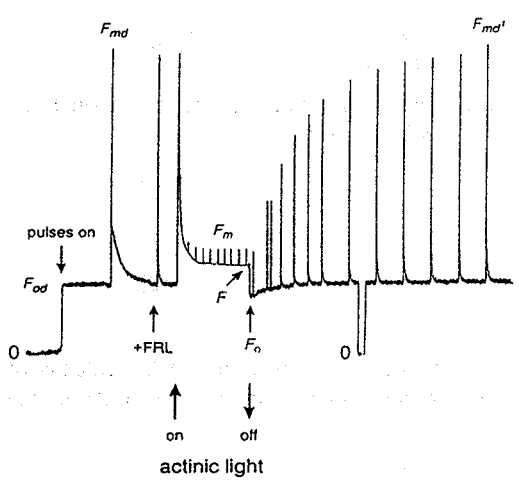

Fig. 5. Fluorescence induction transient (Kautsky effect). An example of fluorescence recording with the PAM fluorometer. A sunflower leaf was dark adapted. F_{0d} is the minimum fluorescence yield obtained in the dark after measurement pulses were turned on. A saturation pulse (8000 μmol quanta m^{-2} s^{-1}) yields the maximum fluorescence in the dark-adapted state, F_{md}. Adding Far-Red light facilitates the re-establishment of F_{0d}. Actinic light (1000 μmol quanta m^{-2} s^{-1}) induces an increase in fluorescence which then decreases again. Under the actinic light, steady state fluorescence yield is F, dark fluorescence yield F_0 is decreased compared with F_{0d} and saturation pulses cause much lower maximum fluorescence, F_m, than in the dark.

high light of 1000 μmol quanta m^{-2} s^{-1}, and still fluorescence did not remain high. This shows that when photochemistry cannot quench excitation at a sufficient rate, a nonphotochemical quencher is induced that quite exactly replaces the disabled or insufficient photochemical quencher, so that fluorescence yield, hence, excitation lifetime, would stay almost constant [9]. The nature of this nonphotochemical quencher has been subject to thorough investigation during the last two decades, and no single mechanism appears to be on its grounds. The above-mentioned regulation of the distances between antenna Chls [8] appears to be responsible for the fastest component of the process (about 1 – 5 min relaxation time), but slower components of the process seem to be related to recombination of charges in the PSII itself.

Simple theory of fluorescence: expressions for quantum yields and rate constants

The above physical principles of fluorescence can be summarized mathematically, using the concept of rate constants for the competing processes, photochemistry (k_P), nonphotochemical, thermal dissipation (k_N) and fluorescence (k_f) [9,10]. For each PSII, together with the surrounding antenna system, one can write the following Eq. (7) for fluorescence yield, when the PSII is in the open state (acceptor oxidized)

$$f_0 = \frac{k_f}{k_f + k_P + k_N}. \qquad (7)$$

For closed PSII that have reduced acceptor, k_P is zero:

$$f_m = \frac{k_f}{k_f + k_N}. \qquad (8)$$

The quantum yield of photochemistry of an open PSII is related to the fluorescence yield as follows:

$$\varphi = \frac{f_m - f_0}{f_m} = \frac{k_P}{k_f + k_P + k_N} \qquad (9)$$

Fluorescence yield of a leaf having a part of PSII closed and the rest open, is a sum of fractional yields

$$F = \left(1 - \frac{N_{IIO}}{N_{II}}\right) \cdot \frac{k_f}{k_f + k_N} + \frac{N_{IIO}}{N_{II}} \cdot \frac{k_f}{k_f + k_P + k_N} \qquad (10)$$

where N_{II} is the total number of PSII per leaf area and N_{IIO} is the number of open PSII. From Eq. 10 one can find the proportion of open PSII as follows:

$$\frac{N_{IIO}}{N_{II}} = \frac{F_m - F}{F_m - F_0} \qquad (11)$$

and the quantum yield of leaf photochemistry

$$Y_{II} = \varphi \frac{N_{IIO}}{N_{II}} = \frac{F_m - F}{F_m} \qquad (12)$$

Eq. 12 is written for isolated PSII, where excitation stays in the limits of the antenna of every individual PSII and cannot jump over to the antenna of the next PSII in the neighborhood (so called puddles model).

Another extreme would be the case of ideally connected PSII, where excitation can easily visit all (at least many) PSII, trying for charge separation in the next when one happens to be closed. In this, so called lake model, the whole family of connected PSII in a leaf forms one multicentral unit, for which Eqs. 7-10 are valid and Eq. 10 can be directly applied for the fluorescence and photochemistry of the whole leaf [11]:

$$Y_{II} = \frac{F_m - F_0}{F_m} = \frac{k_P}{k_f + k_P + k_N} \qquad (13)$$

In Eq. 13 k_P is no more a characteristic of one PSII but is a rather complex expression from the number of open and closed PSII centers. When all centers are closed,

Eq. 10 is converted into

$$F_m = \frac{k_f}{k_f + k_N} \qquad (14)$$

when all centers are open then

$$F_0 = \frac{k_f}{k_f + k_{P0} + k_N} \qquad (15)$$

where k_{P0} now denotes the value for k_P when all centers are open.

Thus, in the lake model the average fluorescence F is formed as a result of averaging k_P not linearly but according to a complex algorithm, while in the puddles model the average F is formed by linearly averaging fluorescence yields of individual PSII.

Eqs. 12 and 13 present the quantum yield of photochemical excitation quenching with respect to quanta absorbed in the PSII antenna. In order to calculate the actual electron transport rate through PSII (J_{II}), the absorbed photon flux density (fluence rate), Q and the fraction of photons delivered to PSII (the relative optical cross-section of PSII, a_{II}) have to be accounted for:

$$J_{II} = a_{II} \cdot Q \cdot \left(1 - \frac{F}{F_m}\right) \qquad (16)$$

and the quantum yield of photochemistry with respect to all absorbed quanta

$$Y_P = a_{II}\left(1 - \frac{F}{F_m}\right) \qquad (17)$$

From Eq. 17 one can see that a_{II} is also equal to the maximum quantum yield of PSII with respect to total incident photons in a hypothetical case when fluorescent losses are absent ($F = 0$). This relationship will be used to determine a_{II} from gas exchange and fluorescence data below. Eqs. 12 and 13 show that the expression for Y_{II} does not depend on the model, whether PSII antennas are perfectly connected lake or not connected puddles, however, the interpretation of the rate constant for photochemistry, k_P, is different. The present understanding of the possible connectivity between PSII centers, which makes it possible for the excitation to reach another center when one is closed, does not allow us to consider that the quantity

$$C_F = \frac{F - F_0}{F_m - F_0} \qquad (18)$$

is a proportional indicator of the fraction of closed centers. If the connectivity is present, then the fraction of closed centers rises more quickly than C_F. Therefore, it is a convention to speak about C_F as the fraction of quanta distributed to closed centers

However, in the puddles model, C_F is a proportional indicator of closed reaction centers.

Instead of the quantum yields Y_{II}, photochemical q_P and nonphotochemical q_N quenching parameters are also widely used:

$$q_P = \frac{F_m - F}{F_m - F_0} \tag{19}$$

$$q_N = \frac{\left(F_{md} - F_{0d}\right) - \left(F_m - F_0\right)}{F_{md} - F_{0d}} \tag{20}$$

These quenching parameters are rather formal since they are not derived on mechanistic basis and are designed only to evaluate the degree to which the variable fluorescence is suppressed. Therefore, in our analyses we do not use these quenching parameters but, rather, quantum yields derived above.

Measurement of the quantum yield of fluorescence

As explained above, fluorescence is a rather easily measurable quantity which is proportional to the presence of excitation energy in the antenna. When all quenching processes have constant probabilities, the intensity of fluorescence is proportional to the incident light. Quantum yield of fluorescence is defined as the ratio of the fluorescence intensity to the absorbed light intensity, both measured as the number of quanta per area per time. Many devices are available to measure fluorescence yield in leaves. Some of these, such as those which require freezing the leaf to 77K, are not suited for simultaneous measurements of fluorescence and photosynthetic gas exchange. In modern chlorophyll fluorometers, fluorescence yield is measured as the fluorescence intensity generated by a constant excitation intensity. These devices provide an excitation beam of constant intensity and measure fluorescence produced only by this beam. In order to measure fluorescence yield simultaneously with photosynthesis, the instrument is made insensitive to the background (actinic) light and to fluorescence produced by it by modulating the measuring beam and detecting only the modulated fluorescence. The modulated measuring beam itself is weak and does not cause additional closure of the reaction centers even in the absence of the actinic light. Thus, the output signal of these instruments is proportional to fluorescence yield from constant excitation, independent of background non-modulated light. One such widely used chlorophyll fluorometer, PAM 101 and the recent portable version PAM 2000, (H. Walz, Effeltrich, Germany) is particularly suited to the requirements of the rapid-response gas exchange system [12,13].

The red light-emitting diode (LED) of the PAM fluorometer excites fluorescence at 650 nm. To avoid interaction between the excitation and measuring beams, the detector is filtered to be sensitive only to the long wavelength tail of fluorescence above 720 nm. A warning has been given that the PAM fluorometer, being sensitive to long-wavelength fluorescence, also sensitively detects the minimum fluorescence emitted from PSI chlorophyll, and this should be considered in data interpretation [14]. In a new version of the instrument, blue LED is used for excitation and the 680 nm fluorescence is preferably sensed. This instrument is free of the deficiency of sensing PSI fluorescence, but instead has a problem that the 680 nm fluorescence is visible only from the very surface layers of the leaf, while the longer wavelengths are emitted from deeper layers also.

We measured fluorescence emission spectra from a sunflower leaf at different quenching states. The F spectra do not show any residual fluorescence at 735 nm when the

680 nm peak extrapolates to zero. Thus, these spectra do not indicate any considerable PSI fluorescence from the leaf [15]. There is a small deviation from the proportionality of 680 and 735 nm peaks in F_m under different nonphotochemical quenching states. Under strongly quenched states the 735 nm peak is relatively higher than the 680 nm peak. On the basis of these spectra the correction of all fluorescence values for $0.3F_0$, as suggested by [14] is not justified.

As explained above, the maximum fluorescence F_m is emitted when PSII reaction centers are closed. Such state can be obtained by applying a very high intensity light pulse, which produces more electrons from PSII than can be consumed due to limitations in the electron transport chain, such as the rate of plastoquinol oxidation and carbon assimilation. A 1-2 s pulse of a very high intensity of about 15000 μmol quanta m^{-2} s^{-1} is needed to reach the full maximum fluorescence yield F_m, but with 8000 μmol quanta m^{-2} s^{-1} un-saturation is still a few per cent.

Fig. 5 shows a demonstration experiment in which fluorescence was recorded with the PAM fluorometer in the course of light-on and light-off transitions with a sunflower leaf at 300 μmol mol^{-1} CO_2 and 1.5 % O_2. The minimum fluorescence F_{0d} of the dark-adapted leaf is best recorded with 1.6 kHz pulse repetition frequency of the measuring beam. A 1s saturation pulse of 8000 μmol quanta m^{-2} s^{-1} closes all PSII reaction centers in the dark-adapted leaf (since further electron transport is completely inhibited by inactivation of the carbon reduction enzymes) and produces the maximum fluorescence yield F_{md}. The subsequent fluorescence transient which occurs when the actinic PFD of 1000 μmol m^{-2} s^{-1} is switched on, shows that this light intensity is also saturating (because further electron transport is completely blocked by inactivated enzymes), giving the same initial fluorescence yield as F_{md}, but this fluorescence quickly decreases. There are two components of this quenching, photochemical and nonphotochemical. The latter is seen from the much lower F_m value produced by the 1s saturation pulse in the presence of the background light. Under light only a part of the PSII centers are closed, as indicated by the positioning of the steady-state fluorescence yield F between F_0 and F_m.

Probing PSI in vivo using absorbance around 800 nm

At room temperature chlorophyll serving for PSI excitation does not emit variable fluorescence. The reason why this is so is not clear. Possibly, in PSI the photochemical excitation capture is so fast that it always largely over-competes fluorescence ($k_P >> k_f$). Unlike PSII, a series of electron carriers are present at the acceptor side of PSI, some of which allow fast charge recombination with the oxidized donor chlorophyll $P700^+$, which usually has a long life-time. Thus, chlorophyll fluorescence cannot be used to monitor PSI function, but, fortunately, there is another possibility.

The donor pigment in the reaction center of PSI is a special pair of chlorophyll P700. Its oxidation state reflects the dynamic interaction of the two photosystems, mediated by the intersystem electron carriers. Just as fluorescence reflects the surplus of quanta and deficiency of e^- acceptor at PSII, P700 oxidation usually reflects the surplus of quanta and deficiency of e^- donor at PSI. In intact leaves, measurements of P700 redox changes at the main absorbance band at 700 nm are complicated by overlapping changes of chlorophyll fluorescence. However, it is possible to measure P700 redox changes with the help of the broad band absorbance increase at 800-830 nm, caused by the $P700^+$ cation radical [16,17].

In this wavelength fluorescence emission and the absorbance of the leaf tissue are small, which makes the 800 nm absorbance change a sensitive indicator of the oxidation of P700.

Absorbance at 800 nm as a probe for P700 reduction state in leaves.

In principle, the absorbance signal around 800 nm is a composite of three signals: P700, plastocyanin and ferredoxin, and other pigments (chlorophylls, the PSII donor P680), all of which have absorption bands in the near infrared region [18]. Fortunately, P680 and chlorophylls do not accumulate in the oxidized form in considerable quantities. Ferredoxin may cause an increase in the 800 nm signal under conditions which lead to acceptor side reduction of PSI, however, its contribution is relatively small and present only in transients when a dark-adapted leaf is suddenly illuminated. The contribution from plastocyanin may theoretically be greater than that from ferredoxin. Because of the difference in redox potentials of plastocyanin and P700 the contribution to absorption changes from these two compounds should not be proportional, and this would make it difficult to interpret the 800 nm measurements in terms of P700 redox changes. However, experiments described below indicate that, in leaves, the sum of the signals from plastocyanin and P700 shows a good linear interrelationship with the quantum yield of PSI, which suggests that plastocyanin does indeed become oxidized approximately in proportion with P700.

The measurements of leaf absorbance near 800 nm were modified by Schreiber and colleagues [19], who incorporated this possibility into the pulse-modulation chlorophyll fluorometer PAM 101, which has made the method available for wide use. For 800 nm measurements the PAM-101 is fitted with a special emitter-detector unit ED800T. As in the case of fluorescence, the pulse-modulated method excludes most of the interference from non-modulated background (actinic) light, but the conditions for 800 nm absorbance measurements are far more strict than for fluorescence measurements. In order to avoid artifacts in P700 measurements, wavelengths above 780 nm must be carefully filtered out from the actinic light source. A new version of the 800 nm detector works on the principle of modulating between two wavelengths, 800/850 nm, what increases the stability of the instrument and decreases the sensitivity to plastocyanin oxidation. Thanks to the low total absorbance and high scattering of radiation in leaves in the near infrared, the 800 nm signal may be measured either in transmission or back-scatter modes. Although the sensitivity to the redox changes of P700 is somewhat better in the back-scatter mode (most of the measuring beam crosses the leaf twice), the transmission arrangement has advantages for measurements with leaves enclosed in a gas exchange chamber (absence of reflections).

The raw output signal of the 800 nm measurements needs to be normalized, and then relative absorbance change is better related to the amount of P700 in the leaf. The 800 nm signal may be converted into per cent change using the following conversion:

$$P(\%) = \frac{P(\mathrm{V})}{g \cdot S_{800}} \qquad (21)$$

where P(V) is the difference between the light (oxidized P700) and dark (reduced P700) levels of the signal in Volts, g is the total gain of PAM 101 plus the external amplifier or recorder, and S_{800} is the maximum 800 nm signal before zeroing the PAM 101 signal with it's offset system.

Calibration of the 800 nm signal for complete reduction and oxidation of P700

Since the useful 800 nm signal is a small differential of about 1% of the total transmission, it is very important to correctly determine reference levels. The two natural reference levels are those that correspond to completely reduced and completely oxidized P700. One can usually be sure that P700 becomes completely reduced in the dark, but the speed of the reduction may be different dependent on the availability of electrons in the interphotosystem pool. From low PADs the complete reduction of P700 will take 30-40 s, while from high PADs it happens within a second.

Establishing the level of the 800 nm signal which corresponds to complete oxidation of P700 is more complicated than establishing the level that corresponds to complete reduction of the pigment. It is commonly assumed that far-red light (710 - 730 nm; further referred to as FRL) produces almost complete oxidation of P700, since it preferably excites PSI. In the presence of FRL electrons may be moved only from the donor side pools of PSI (plastoquinol, cytochrome b_6f , plastocyanin, P700) into the acceptor side pools (ferredoxin, NADPH). Further movement to the CRC depends on the presence of ATP. P700 can be photo-oxidized by FRL only in those PSI complexes that have open (oxidized) acceptor side. Oxidation of the acceptor side of PSI is principally dependent on the availability of 3-phosphoglycerate (PGA) and ATP, the substrates for the PGA kinase to produce the electron acceptor 1, 3-bisphosphoglycerate (BPGA), but direct photoreduction of nitrite and O_2 are also possible. If FRL energizes cyclic electron flow around PSI, some ATP may be produced that helps to reduce PGA and to remove electrons from NADPH and ferredoxin. Experiments show that in many cases, especially after strong reducing conditions were applied, P700 cannot be completely oxidized in the dark under FRL, which indicates that poor conditions for further electron transport may be present under FRL (e.g., not enough ATP may be available). This means that even under FRL the acceptor side of some PSI complexes may stay reduced, which causes underestimation of the maximum 800 nm difference signal P_m measured under FRL. The useful 800 nm signal, P, is the difference between the measured level and the dark level, where P700 is reduced. P_m corresponds to the maximum level, when all P700 is oxidized, while P_o corresponds to the oxidizable P700 (P_m-P_o corresponds to those PSI that have closed acceptor side).

Technically, FRL can be obtained with an interference filter with a maximum at 720 nm, 10 nm bandwidth or an appropriate combination of wide-band filters. Even the most carefully filtered FRL causes about 10-15% excitation of PSII compared with the excitation of PSI. Therefore, a correction factor must be applied to the signal obtained under FRL to obtain the maximum 800 nm signal difference P_m corresponding to the complete oxidation of P700. It may be calculated from the excitation/electron budget of PSI and usually

$$P_m = 1.12 P_{FRL} \qquad (22)$$

where P_m is the maximum deflection of the 800 nm signal from the dark level, corresponding to completely oxidized P700 and P_{FRL} is the deflection measured under far-red light. Dependent on the used filter, the coefficient may vary.

We also have used high-intensity pulses of white light to maximally oxidize P700. Short high-intensity pulses of white light of ms duration ensure that the measurement can be completed before the fast flux of electrons generated by PSII during the pulse arrives at $P700$ via the cytochrome b_6f complex. The authors of the method [20] warn that the signal from the standard ED 800T detector is influenced by the very high chlorophyll fluorescence

generated by the pulse. In our measurements this influence was no more than 10% of the P_m value and was considered.

Excitation and electron budget in photosynthesis

In photosynthesis electrons are transported sequentially through PS II and PS I at the expense of light energy, while between the two photosystems plastoquinone and plastocyanin are diffusible electron carriers and electron/proton cotransport is accomplished by the Cyt b_6f complex. For the maximum efficiency of the whole chain a certain distribution of excitation between the two photosystems and fast operation of Cyt b_6f are required. The partitioning of energy between the photosystems is governed by the ratio of e^- fluxes through PS II and PS I [21]

$$\frac{a_{II}}{n_{II}}\left[\frac{F_m - F}{F_m}\right] = \frac{a_I}{n_I}\left[\frac{P_o - P}{P_m}\right] \tag{23}$$

and by the budget of absorbed quanta

$$a_{II} + a_I + a_0 = 1 \tag{24}$$

where a are the relative optical cross-sections (quantum partitioning ratios) to the given photosystem (as indicated by the subscript) and n is the number of e^- required to pass through the given photosystem for a given process (e.g. per CO_2 fixed or O_2 evolved); F and F_m are steady-state and pulse-saturated fluorescence yields respectively of PSII, P and P_m are 800 nm signals reflecting the steady-state and maximum oxidation of $P700$, the donor pigment of PS I, and P_o is the oxidizable part of $P700$ corresponding to open PS I centers. The terms in square brackets represent the efficiencies of excitation use at the photosystems (sometimes denoted as Φ), the relative photochemical quenching of fluorescence indicating the efficiency of PS II and the relative reduction state of the oxidizable $P700$ indicating the efficiency of PS I. The efficiency of excitation use by PS I for charge separation is considered to be close to one. Only these PS I centers are considered efficient in electron transport that have reduced donor side and oxidized acceptor side (P_o-P). If a fraction of the centers have reduced acceptor side and, correspondingly, reduced donor side (P_m-P_o), they would be inefficient even though they have reduced P700. In the quantum budget (Eq. 24) the term a_0 accounts for quanta absorbed in non-photosynthetic structures or pigments and quanta supporting reductions not visible in the measured process, such as Mehler type O_2 reduction in O_2 and CO_2 measurements and N reduction in CO_2 measurements. Solving Eqs. 23 and 24 for an optimal case of $(F_m$-$F)/F_m = 0.8$ and $(P_o$-$P)/P_m = 1$, $n_I = n_{II} = 4$ and $a_0 = 0.05$ reveals that the maximum theoretical quantum yield for O_2 evolution is 0.105 with optimal cross-section values of $a_{IIO2} = 0.53$ and $a_{IO2} = 0.42$ (O_2 is added in the subscript to indicate that these cross-sections support O_2 evolution). This is also the experimental value obtained for quantum yields based on net O_2 evolution for 37 species under nonphotorespiratory conditions [22,23]). If Eqs. 23 and 24 are solved for CO_2 uptake measurements under nonphotorespiratory conditions, then a_0 is larger due to other assimilatory processes-particularly nitrogen, and a_I and a_{II} will be correspondingly lower, meaning that the optical cross-sections supporting CO_2 fixation are smaller than those supporting O_2 evolution, the difference supporting alternative reductions of N and O_2. Solving Eqs. 23 and 24 with $a_0 = 0.15$, the maximum quantum yield of CO_2 assimilation would be 0.095, with $a_{II} = 0.47$ and $a_I = 0.38$. Maximum experimental quantum yields of C_3 plants under nonphotorespiratory

conditions are again close to this, though experimental variation is greater: 0.073 ±0.001 (seven *Atriplex*, *Encelia* and *Plantago* species, [24]; 0.087 for sunflower [25] and 0.093 for 11 species of diverse taxa [26].

C_4 plants, such as maize, sorghum, amaranth etc. require production of 2 ATP for the C_4 cycle through PSI dependent cyclic e^- flow, in addition to the 3 ATP used for carbon reduction and produced from linear electron flow. With a requirement of 4 H^+/ATP (Rumberg et al. 1990), 8 H^+ would be needed per CO_2 fixed and with utilization of 4H^+ per ATP a flux of 8 e^- would be required through PS I per CO_2 fixed, versus 4 e^- through PS II. In this case the value of n_I in Eq. 23 would be 8, while n_{II} is 4. Four additional e^- would need to be cycled through PS I per CO_2 fixed to produce the two additional ATP and for a balanced operation, the PS I antenna would have to be almost double the size of the PS II antenna in C_4 plants. Applying $n_I = 8$ in Eq. 23, the integral quantum yield of C_4 plants would be 0.073, $a_{II} + a_I = 0.95$, $a_{II} = 0.365$, $a_I = 0.585$. Our experiments (below) have shown that the actual quantum yield of C_4 plants is higher than predicted by this theory.

Experimental Results

The above theoretical considerations showed how chlorophyll fluorescence and 800 nm absorbance measurements can be used for the analysis of excitation budget in photosynthesis. These optical measurements help to determine losses of quanta that occur at both photosystems, allowing to put together a correct excitation budget. The basic method for data presentation to determine optical cross section values to support CO_2 fixation is such where e^- transport rate (or quantum yield of e^- transport) calculated from the measurements of CO_2 uptake are plotted against the quantum yield of PSII calculated from fluorescence or of PSI calculated from 800 nm data.

Calculation of electron transport from CO_2 exchange

In C_3 plants, in the absence of photorespiration, e^- transport rate can be calculated as four times CO_2 fixation rate. However, photorespiration is always present, even at 1-2% O_2, and this can be considered if e^- transport is calculated using Eq. 25 [27]:

$$J_C = 4(A + R_d)\cdot\frac{2K_s\left[C_{w0} - (r_{gw} + r_{md})A\right] + nO_{w0}/4}{2K_s\left[C_{w0} - (r_{gw} + r_{md})A\right] - O_{w0}} \qquad (25)$$

where A is the measured net assimilation rate, R_d is dark respiration rate in the light, K_s is Rubisco specificity factor (K_s = 90, [27]), C_{w0} and O_{w0} are molar CO_2 and O_2 concentrations in liquid phase, equilibrated with the external gaseous CO_2 and O_2 concentration (O_{w0} = 15 μM, C_{w0} = 30 μM in experiments below), r_{gw} and r_{md} are leaf gas phase and liquid phase diffusion resistances, respectively, as calculated from leaf transpiration and photosynthesis rates, and n (= 8) is the number of e^- in linear e^- transport required per CO_2 evolved from photorespiration. For C_4 plants with little photorespiration Eq. 25 simplifies as then one may assume that K_s is infinity.

Measurement of light response curves of CO_2 exchange, fluorescence and 800 nm transmission

A typical recording of CO_2 exchange, fluorescence and 800 nm signal during the measurement of the light response curves is shown in Fig. 6. After the photosynthetic rate

had stabilized at a given PAD, a pulse was given, to obtain pulse-saturated levels of fluorescence and 800 nm signal. F_m was read at the maximum during the flash, P_o was obtained as the maximum deflection of the 800 nm signal from the dark level during the flash. Thereafter light was switched off for 4 s to obtain the dark level of the 800 nm signal, then FRL was switched on for 4 s to oxidize interphotosystem carriers, and off again, to measure dark fluorescence F_0. After these procedures photosynthesis was stabilized at the next actinic PAD. The stabilization time was about 3 - 5 min at each PAD (this time is about 1 min in Fig. 1, made especially shorter for demonstration purposes). The maximum deflection under FRL, P_{FRL}, was measured in the absence of white light and the deflection corresponding to completely oxidized P700 was calculated from Eq. 22.

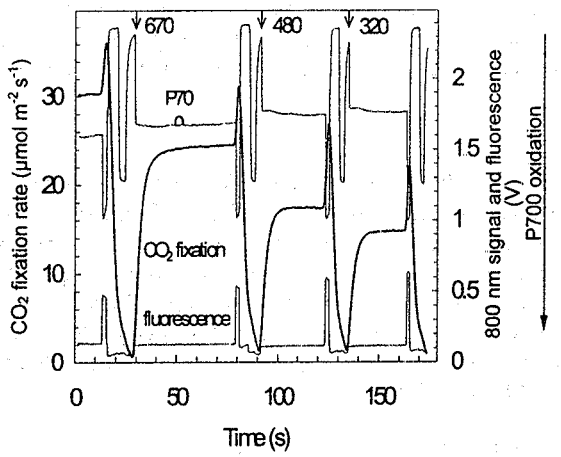

Fig. 6. Computer-recorded traces of a segment of the measurement of light response curves. CO_2 fixation rate, thick line and left ordinate; 800 nm signal, upper thin line and right ordinate; fluorescence yield, lower thin line and right ordinate. The recording begins at a PAD of 880 μmol m^{-2} s^{-1}. At time = 14 s a 2 s pulse of 10500 μmol m^{-2} s^{-1} (down in 800 nm signal, up in fluorescence signal) followed by darkness for 4 s (up in 800 nm), FRL for 4 s (down in 800 nm), darkness for 4 s (up in 800 nm) and the next PAD of 670 μmol m^{-2} s^{-1}. The routine is repeated at the following two PADs of 480 and 320 μmol m^{-2} s^{-1}.

Quantum yield and fluorescence

Electron transport rates were calculated from CO_2 exchange rate (Eq. 25) and the quantum yield of PSII electron transport was plotted against $(F_m - F)/F_m$ (Fig. 7A). For tobacco, the relationship is linear, there is no deflection from linearity that could be related to the presence of an alternative e^- transport or state transition in these leaves. Extrapolation of the relationships to the axis of ordinate that presents the relative excitation (optical cross-section) of PSII $a_{II} = 0.51$, but it may vary dependent on plants.

Quantum yield and 800 nm transmission

The 800 nm signal difference between the light and dark levels continuously increased (more oxidation of P700) over the whole range of increasing light. The 800 nm data are presented by plotting the quantum yield Y vs. $(P_o-P)/P_m$ (Fig. 7B), a presentation of the quantum yield of PSI which is similar to the presentation of Y vs. $(F_m-F)/F_m$ for PSII (Fig. 7A). Typical P_m values for tobacco plants were 1.20% for high light and0.89% for low light

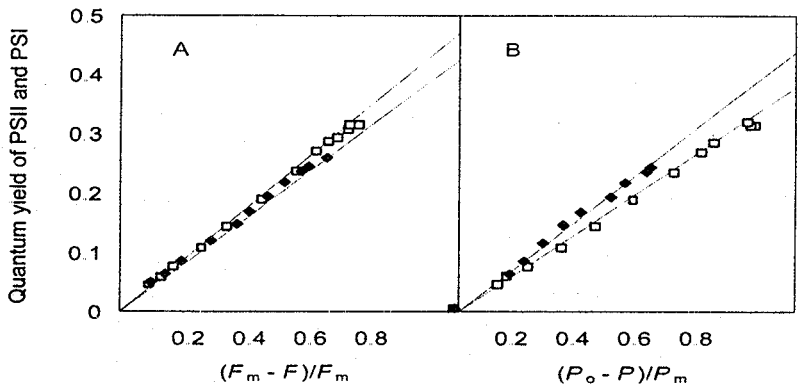

Fig. 7. Quantum yield of PSII electron transport calculated from CO_2 assimilation as a function of $(F_m-F)/F_m$ (panel A) and quantum yield of PSI electron transport calculated from CO_2 assimilation as a function of $(P_o-P)/P_m$ (panel B). Empty squares – high light grown tobacco, filled diamonds – low light grown tobacco.

grown plants. The relationships of Y vs. $(P_o - P)/P_m$ were very close to straight lines, which shows that e^- transport through Cyt b_6/f was the major bottleneck under the conditions of these experiments. These lines (dotted lines in Fig. 7B) extrapolate to P_o on the abscissa, the intercept corresponding to all oxidizable P700, and to a_I on the ordinate, the relative optical cross-section of PSI. In these leaves the difference between P_o and P_m was not detectable, since non-oxidizable P700 (PSI with acceptor side reduced) were practically absent. Extrapolation of the plots in Fig. 7B to the axis of ordinates yields values of the relative optical cross-section of PSI, a_I, about 0.38 for the high light and 0.45 for the low light grown tobacco.

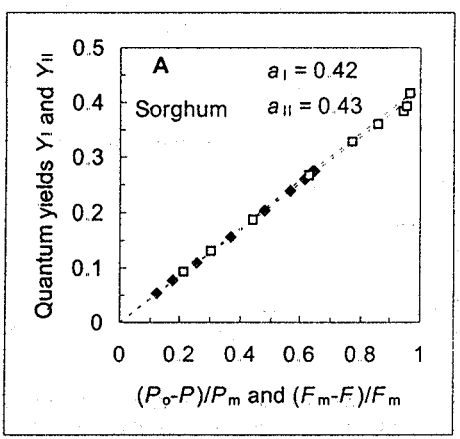

Fig. 8. Electron transport rates and quantum yields of PS I and PS II e^- transport in experiments with sorghum. Quantum yield of PS I, Y_I, was calculated from CO_2 fixation assuming $n_I = 6$ and plotted against the quantum yield of PS I calculated from 800 nm transmission measurements (empty squares). Quantum yield of PS II, Y_{II}, was calculated from CO_2 fixation using $n_{II} = 4$ and plotted against the quantum yield of PS II calculated from fluorescence measurements (filled diamonds).

C_4 plants

Similar data for a C_4 plant sorghum are shown in Fig. 8. We tested different values of n_I for calculation of Y_I (Eq. 6) in C_4 plants, and concluded that $n_I = 6$ gives the best fit in the quantum budget. The results indicate that the absorption cross section values supporting CO_2 fixation in C_4 plants are lower for PSII and higher for PSI than in C_3 plants; whereas, the sum of the absorption cross section use is similar. The average values from replicated experiments were $a_I = 0.44 \pm 0.01$ and $a_{II} = 0.45 \pm 0.01$ for sorghum, $a_I =$

0.45±0.02 and a_{II} = 0.44±0.02 for amaranth, and a_I = 0.36±0.02 and a_{II} = 0.48 ±0.02 for sunflower (a C_3 species).

Thus, in C_4 plants, a_I and a_{II} were approximately equal (about 0.45), but in the C_3 plants, a_{II} was considerably greater than a_I, which reflects differences in the energetics of CO_2 fixation between C_3 and C_4 species. In C_3 plants, the sum of $a_I + a_{II}$ = 0.84, which results in an a_0 value of 0.16, and indicates 16% cross-section is available for residual photorespiration at 1.5% O_2, alternative reductions and absorption by non-photosynthetic pigments. In C_4 plants, with a PS I requirement of 6 e^-/CO_2, the sum of $a_I + a_{II}$ = 0.89, which results in a slightly smaller residual optical cross-section a_0 than in the C_3 species. If 8 instead of 6 e^- were transported through PS I per CO_2 assimilated in C_4 plants, the necessary optical cross-section of PS I to support CO_2 assimilation increases proportionally, to a_I = 0.60, and the sum of $a_I + a_{II}$ = 1.05 ±0.03. Again, allowing for other optical cross-sectional use, a_0, the quantum budget of the leaf would be $a_I + a_{II} + a_0$ = 1.15, which clearly exceeds the maximum of 1.0. Thus, a PS I activity of 6 e^-/CO_2 provides the best fit for the quantum budget in C_4 plants, in good accordance with that in C_3 plants, while 8e^-/CO_2 is energetically impossible.

Postillumination rereduction of P700

P700 is largely oxidized in high light, but plastoquinone is reduced due to the rate-limiting resistance imposed by Cyt b_6f. After light is removed, electrons from plastoquinone continue to flow through Cyt b_6f and to reduce P700. The speed of this reduction can be recorded as a change in the 800 nm signal and it characterizes the electron

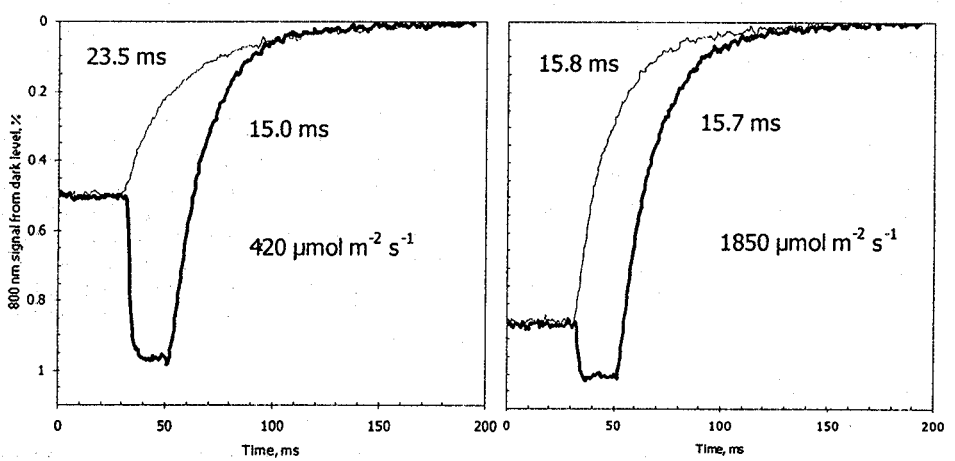

Fig. 9. Measurement of P700 rereduction rate without and with a pre-illumination pulse. Actinic illumination was interrupted at Time = 30 ms and the P700 rereduction kinetics were recorded as a transient in the 800 nm signal (thin line). In another version of the experiment a 10 ms pulse of 13500 µmol quanta m^{-2} s^{-1} was given before the light was turned off (thick line). P700 rereduction time constants are shown at the curves, as well as the steady-state actinic illumination PAD for experiments in panels A and B.

transport resistance in Cyt b_6f. A methodical problem with these measurements is that at low PADs PQ may be oxidized and e^- are not available for fast P700 reduction. If this is so, the P700 reduction rate is limited by low PQH_2 pool but not the turnover rate of Cyt b_6f. To

overcome this problem, a short pulse of white light is given before light is turned off (Fig. 9). With the pulse pre-illumination, the P700 rereduction time characterizes the maximum turnover rate of Cyt b_6f.

The slope of the graph where electron transport rate is plotted against the rate constant of P700 rereduction ($k_c=1/\tau$) represents the number of P700 that participate in electron transport [28]. Our data with wild type and Cyt b_6f deficient transgenic tobacco [21] fall into two categories, suggesting that leaves with two different PS I population densities exist (Fig. 10). The histogram (insert in Fig. 10) was calculated from the relationship $N_I = k_c/J$ (N_I, the number of PS I centers, J, electron transport rate) using data for many leaves of different treatments. Two peaks, one at N_I=1.2, the other at 2.2 μmol m^{-2} are resolved. Plants with lower PS I density were mostly (80%) low-light grown antisense and high-light grown wild-type.

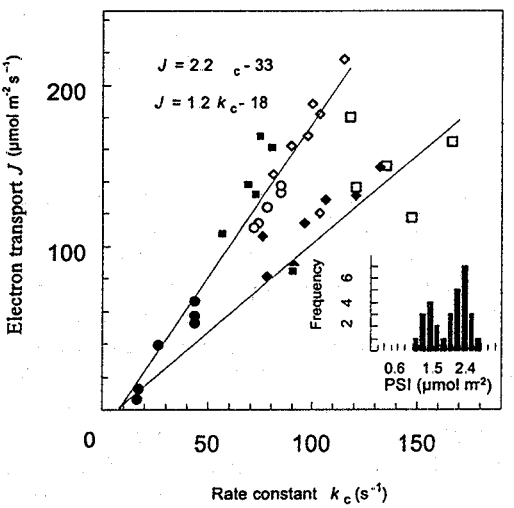

Fig. 10. PSI electron transport rate as a function of the PSI donor side rate constant $k_c = 1/\tau$(τ, time constant for P700 rereduction). Differently grown wild type and Cyt b_6f deficient transgenic tobacco plants. Inserted: frequency distribution of numbers of PS I centers active in electron transport, calculated from the electron transport rate and donor side resistance. The two maximums are at 1.2 and 2.2 μmol m^{-2} of PSI centers.

Fluorescence induction and O_2 evolution during multiple turnover pulses: the effect of PSII donor side resistance

Chlorophyll fluorescence is a reliable quantitative indicator of steady state e^- transport rate. Since processes leading to fluorescence emission are completed within nanoseconds, there is no reason to doubt that fluorescence should not be as good a quantitative indicator of e^- transport during multiple turnover pulses of ms duration. An important difference between the transient and steady-state process is that e^- transport in pulses is extremely fast compared with the steady state, if a pulse is applied in the state where PQ is oxidized. Then PSII e^- transport is limited only by transfer processes on the donor and acceptor side and these are faster than one ms. Under this condition the accumulation of $P680^+$ that usually is unimportant, may become important. In the following experiments we compared the total O_2 yield from pulses with the integral of e^- transport calculated from fluorescence induction during the same pulses. Fluorescence was measured with a PAM 101 fluorometer. Electron transport rate was calculated using Eq. 16, where F was time-dependent.

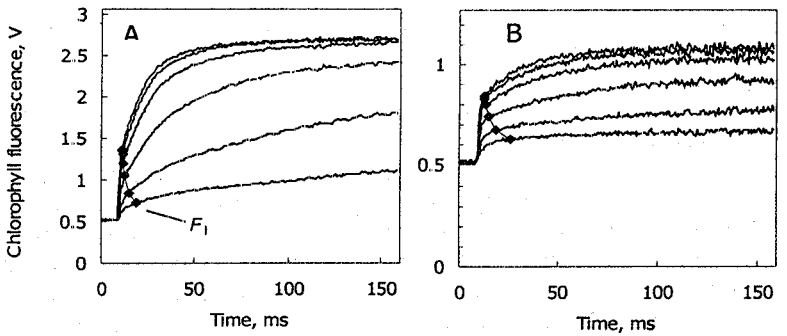

Fig. 11. Fluorescence induction curves in a low light (A) and high light (B) adapted sunflower leaf. In the beginning of traces fluorescence yield corresponds to F_0, the upper limit of the plot area corresponds to F_m (=3.06V in A and 1.27 V in B). The fast increase of fluorescence corresponds to the beginning of the light pulse. Marked points correspond to fluorescence denoted F_i when 3 μmol e^- m^{-2} have been transferred to reduce bound acceptors; further on free plastoquinone is reduced. Pulse PADs were (downward for curves) 13500, 10200, 6800, 3600, 1720 and 880 μmol m^{-2} s^{-1}.

Fluorescence induction transients recorded during pulses of different intensities in leaves preconditioned to low and high PAD are shown in Fig. 11. In dark-adapted leaves the induction was a complex curve with a minimum (not shown) but adaptation to PAD of 60 μmol m^{-2} s^{-1} or higher eliminated the minimum and the induction became approximately exponential. Electron transport during the pulses (J_F) was calculated using simultaneously recorded data points of fluorescence and pulse PAD and an F_m value measured at the end of a separate 1s pulse of 13500 μmol quanta m^{-2} s^{-1}. This F_m (3.06 V in A and 1.27 V in B, corresponds to the upper limit of the plot area), was higher than that reached at the end of 160 ms pulses in Fig. 11, because ETR through PS II was still fast during the pulse.

The calculated values of J_F were integrated point by point to find the total e^- transport during a pulse of a given length, which then was compared with the measured total O_2 evolution during the same pulse. Pulse totals of the calculated e^- transport and measured O_2 evolution were proportional to one another when pulse length was increased at constant PAD, but the slope of the relationship (e^- from fluorescence/e^- from O_2 evolution, J_F/J_O) was dependent on pulse PAD (Fig. 12A,B). In pulses of low PAD, where ETR was slow, J_F/J_O was close to one independent of pre-adaptation conditions, but in pulses of high PAD that caused fast e^- transport J_F/J_O was much higher than one.

Thus, Eq. 16 well describes the relationship between fluorescence and PS II e^- transport during fluorescence induction at physiological ETR values, but it progressively overestimates J_O when PAD becomes much higher than physiological and ETR increases during short pulses. These results suggest that there is a fraction in F_m-$F(t)$ that is quenched, but not photochemically, because it is not accompanied by corresponding e^- transport. Quite evidently, this fraction is quenched by $P680^+$, the PS II donor pigment that accumulates in oxidized form in the presence of the very fast e^- transport from oxygen evolving complex (OEC) to PQ during the high-intensity pulses. An empirical formula that describes the relationship between fluorescence and e^- transport in the presence of $P680^+$ can be found from our data, considering that the amount of $P680^+$ is proportional to e^-

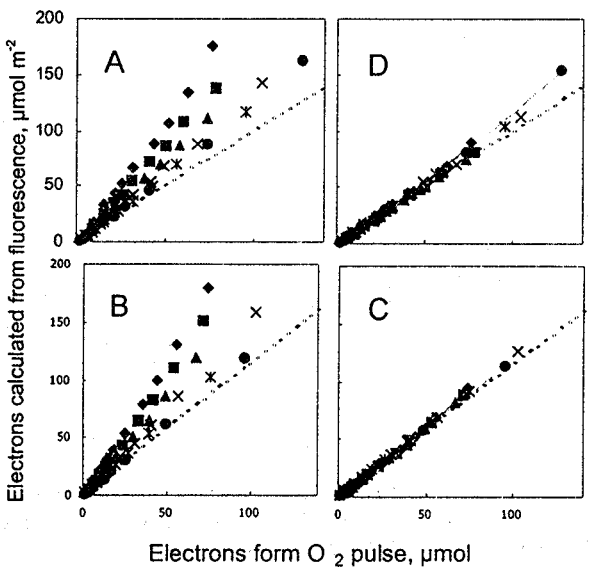

Fig. 12. Total per pulse of electrons calculated from fluorescence related to total per pulse of electrons calculated from O_2 evolution when pulse length was varied from 5 to 160 ms in a low light (A, D) and high light (B, C) adapted sunflower leaf. Donor side resistance r_d in Eq. 26 was assumed to be 0 (A, B) or 0.00014 s m^2 μmol^{-1} (D, C). Data from the experiment in Fig. 11. Pulse PADs were 13500 (diamonds), 10200 (squares), 6800 (triangles), 3600 (crosses), 1720 (asterisks) and 880 (circles) $\mu mol\ m^{-2}\ s^{-1}$.

transport rate and the proportionality constant may be expressed as PSII donor side resistance [29]:

$$J_F^{'} = J_O = a_{II} Q \frac{F_m^{'} - F(t)}{F_m^{'}} \cdot \frac{1}{1 + a_{II} r_d Q} \qquad (26)$$

Compared with Eq. 16, Eq. 26 contains an additional parameter r_d, which characterizes the donor side resistance of PS II per unit leaf area. The quality of Eq. 26 for the calculation of fast ETR through PS II is demonstrated in Fig. 12 C and D, where one and the same donor side resistance r_d of 0.00014 $\mu mol^{-1}\ m^2$ s was applied for all pulse lengths and PADs and for both, low and high light adapted states.

Time course of PSII electron transport calculated from fluorescence

Time courses of electron transport were calculated from fluorescence induction curves applying Eq. 26 considering the donor side re-reduction time. In Fig. 13 the data are plotted against the cumulative amount of electrons transported into the PQ pool, an integral of J_F calculated from all recorded data points. After the rising edge of the pulse passed, fluorescence increased immediately and continued to increase (Fig. 11). Correspondingly, the calculated electron transport rate decreased from the beginning of the pulse (Fig. 13). This was unexpected since it did not agree with the assumption that PQ reduction had a small reverse effect on the Q_A reduction due to the more negative redox potential of the latter, but, rather, indicated that in the light-adapted state the medium point redox potentials of Q_A and free PQ are almost equal. The initial electron transport rate from OEC to completely oxidized PQ pool, J_{Fi} was obtained as the electron transport rate after the first 3 $\mu mol\ e^-\ m^{-2}$ were transported (shown with a dotted line in Fig. 13). The first 2-3 $\mu mol\ e^-m^{-2}$ were transported at a higher rate, as well seen from Fig. 13B, evidently because they

reduced Q_A and bound PQ (Q_B) and were not exchanged with the free PQ pool. The initial rate of PS II electron transport J_{Fi} reached about 2000 μmol m^{-2} s^{-1} for the maximum pulse

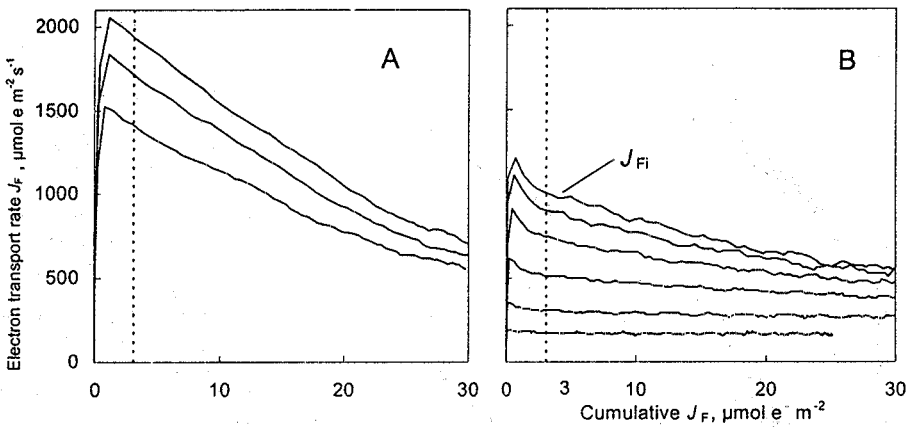

Fig. 13. Electron transport rate during light pulses calculated from Eq 26 as a function of cumulative electron transport in a sunflower leaf adapted to 60 (Panel A) and 2000 (Panel B) μmol quanta m^{-2} s^{-1}. Pulse PADs were (downward for curves) 13500, 10200, 6800, 3600, 1720 and 880 μmol m^{-2} s^{-1}. The initial electron transport rate J_{Fi} was read after 3 μmol e^- m^{-2} were transported (at the dotted line).

PAD in the low light adapted state, but was clearly lower (1000 μmol e^- m^{-2} s^{-1}) in the high light adapted state.

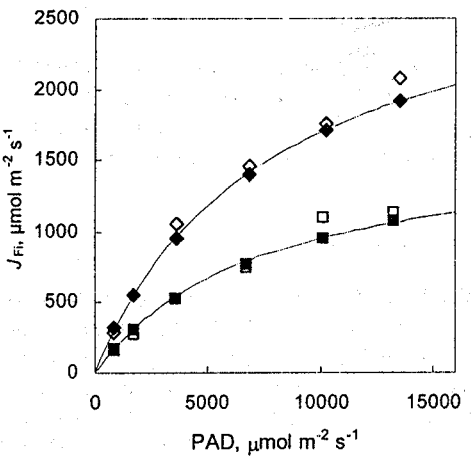

Fig. 14. Light response curves of the initial electron transport into oxidized plastoquinone pool, J_{Fi} in sunflower leaves (filled symbols). Diamonds, low light adapted leaf; squares, high light adapted leaf (data from Fig. 13); open symbols, data from the O_2 evolution rate; lines are rectangular hyperbolae calculated from the mathematical model of PS II electron transport.

PS II light response curves were obtained by plotting J_{Fi} values from Fig. 13 against pulse PAD (Fig. 14, filled squares). The light response curves of PS II electron transport were rectangular hyperbola, and very well fit with the O_2 evolution data, however, scattering of J_{Fi} calculated from fluorescence was considerably less than the scattering of J_{Oi} calculated from O_2 evolution. Considering that there were 2 μmol PS II m^{-2} [29] and using the extrapolated J_{Fm} values we calculated that the average electron transfer time from OEC through PS II to PQ increased from 700 to 1380 μs when the nonphotochemical excitation quenching q_N increased from the minimum to the maximum. Thus, these experiments show that PSII maximum turnover rate (maximum electron transport capacity) decreases in the presence of nonphotochemical excitation.

The type of the quenching in our experiments was mostly reversible photoinhibitory type q_I, not the energy-dependent q_E type, because the leaves were pre-conditioned at the high PAD for 90 min.

Summary

Chlorophyll fluorescence and transmission at 800 nm are two easily measurable optical signals from intact leaves that characterize the function of PSII and PSI, respectively. When measured together with CO_2 uptake or O_2 evolution, important characteristics of the leaf photosynthetic machinery can be calculated if the data are properly analyzed: fractions of quanta lost at PSII and PSI separately, relative optical cross-sections of PSII and PSI, the number of PSI per leaf area, the maximum turnover rate of PSII, the turnover rate of cytochrome b_6f complex, changes in PSII turnover rate as influenced by nonphotochemical excitation quenching. Such complex measurements allow to diagnose the state of leaves in natural ecosystems and the changes introduced into the photosynthetic machinery by transgenic interference.

Acknowledgement. This work was supported by Estonian Science Foundation Grant 3907.

Agu Laisk is professor of plant physiology, Institute of Molecular and Cell Biology, University of Tartu, Estonia (23 Riia St., 51010 Tartu, Estonia)

References

1. Edwards, G. and Walker, D.A. (1983) C_3,C_4: mechanisms, and cellular and environmental regulation, of photosynthesis. Blackwell, Oxford, London.

2. Renger, G. (1992) Energy transfer and trapping in photosystem II. *In* Topics in Photosynthesis, Vol. 11. The Photosystems: Structure, Function and Molecular Biology. (J. Barber, ed.), pp. 45-100, Elsevier, Amsterdam-London-New York-Tokyo.

3. Holzwarth, A.R. and Roelofs, T.A. (1992) Recent advances in the understanding of chlorophyll excited state dynamics in thylakoid membranes and isolated reaction centre complexes. Photochem. Photobiol. B: Biol. 15, 45-62.

4. Bassi, R., Marquardt, J. and Lavergne, J. (1995) Biochemical and functional properties of photosystem II in agranal membranes from maize mesophyll and bundle sheath chloroplasts. Eur. J. Biochem. 233, 709-719.

5. Govindjee (1995) Sixty-three years since Kautsky: Chlorophyll a fluorescence. Aust. J. Plant Physiol. 22, 131-160.

6. Valkunas, L., Liuolia, V., Dekker, J.P. and van Grondelle, R. (1995) Description of energy migration and trapping in photosystem I by a model with two distance scaling parameters. Photosynth. Res. 43, 149-154.

7. van Mieghem, F., Brettel, K., Hillmann, B., Kamlowski, A., Rutherford, W.A. and Schlodder, E. (1995) Charge recombination reactions in photosystem 2. 1. yields, recombination pathways, and kinetics of the primary pair. Biochemistry 34, 4798-4813.

8. Horton, P. and Ruban, A.V. (1992) Regulation of photosystem II. Photosynth. Res. 34, 375-385.

9. Laisk, A., Oja, V., Rasulov, B., Eichelmann, H. and Sumberg, A. (1997) Quantum yields and rate constants of photochemical and nonphotochemical excitation quenching. Experiment and model. Plant Physiol. 115, 803-815.

10. Lavergne, J. and Trissl, H.-W. (1995) Theory of fluorescence induction in photosystem II: Derivation of analytical expressions in a model including exciton-radical-pair equilibrium and restricted energy transfer between photosynthetic units. Biophys. J. 68, 2474-2492.

11. Genty, B., Briantais, J.M. and Baker, N.R. (1989) The relationship between quantum yield of photosynthetic electron transport and quenching of chlorophyll fluorescence. Biochem. Biophys. Acta 990, 87-92.

12. Schreiber, U., Bilger, W. and Schliwa, U. (1986) Continous recording of photochemical and non-photochemical chlorophyll fluorescence quenching with a new type of modulation fluorometer. Photosynth. Res. 10, 51-62.

13. Schreiber, U., Neubauer, C. and Klughammer, C. (1989) Devices and methods for room-temperature fluorescence analysis. Phil. Trans R. Soc. Lond. B. 323, 241-251.

14. Genty, B., Wonders, J. and Baker, N.R. (1990) Non-photochemical quenching of F0 in leaves is emission wavelength dependent: consequences for quenching analysis and its interpretation. Photosynth. Res 26, 133-139.

15. Laisk A. and Oja V. (1998) Dynamic gas exchange of leaf photosynthesis. Measurement and interpretation. CSIRO Publishing, Canberra.

16. Genty, B. and Harbinson, J. (1996) Regulation of light utilization in photosynthetic electron transport. *In* Photosynthesis and the Environment. (Baker, N.R., ed) pp. 67-99, Kluwer Acad. Publ., The Netherlands.

17. Kramer, D.M. and Crofts, A.R. (1996) Control and measurement of photosynthetic electron transport. *In* Photosynthesis and the Environment. (Baker, N.R. ed), pp. 25-66, Kluwer Acad. Publ., The Netherlands.

18. Klughammer, C. and Schreiber, U. (1991) Analysis of light-induced absorbance changes in the near-infrared spectral region. I. Characterization of various components in isolated chloroplasts. Z. Naturforsch. 46c, 233-244.

19. Schreiber, U., Klughammer, C. and Neubauer, C. (1988) Measuring P700 absorbance changes around 830 nm with a new type pulse modulation system. Z. Naturforsch. 43c, 686-698.

20. Klughammer, C. and Schreiber, U. (1994) An improved method, using saturating light pulses, for the determination of photosystem I quantum yield via $P700^+$-absorbance changes at 830 nm. Planta 192, 261-268.

21. Eichelmann, H. and Laisk, A. (1999) Cooperation of photosystems II and I in leaves as analysed by simultaneous measurements of chlorophyll fluorescence and transmittance at 800 nm. Plant Cell Physiol. (submitted).

22. Demmig, B. and Björkman, O. (1987) Comparison of the effect of excessive light on chlorophyll fluorescence (77K) and photon yield of O_2 evolution in higher plants. Planta 171, 171-184.

23. Lal, A. and Edwards, G.E.E. (1995) Maximum quantum yields of O_2 evolution in C_4 plants under high CO_2. Plant Cell Physiol. 36, 1311-1317.

24. Ehleringer, J. and Björkman, O. (1977) Quantum yields for CO_2 uptake in C_3 and C_4 plants. Plant Physiol. 59, 86-90.

25. Sharp, R.E., Matthews, M.A. and Boyer, J.S. (1984) Kok effect and the quantum yield of photosynthesis. Light partially inhibits dark respiration. Plant Physiol. 75, 95-101.

26. Long, S.P., Postl, W.F. and Bolhar-Nordenkampf, H.R. (1993) Quantum yields for uptake of carbon dioxide in C_3 vascular plants of contrasting habitats and taxonomic groupings. Planta 189, 226-234.

27. Laisk, A. and Sumberg, A. (1994) Partitioning of the leaf CO_2 exchange into components using CO_2 exchange and fluorescence measurements. Plant Physiol. 106, 689-695.

28. Laisk, A. and Oja, V. (1994) Range of the photosynthetic control of postillumination P700 reduction rate in sunflower leaves. Photosynth. Res. 39, 39-50.

29. Oja, V. and Laisk, A. (1999) Electron transport through photosystem II in leaves during light pulses: quantification of the donor resistance. Biochim. Biophys. Acta (submitted).

30. Nobel, P.S. (1991) Physicochemical and environmental plant physiology. Academic Press, Inc., San Diego.

Institute for Molecular and Cell biology
University of Tartu
Riia str. 23
EE-51010 TARTU, Estonia